JOURNAL OF COMPUTATIONAL PHYSICS **127,** 118–127 (1996)
ARTICLE NO. 0162

Thermodynamically Consistent Interpolation for Equation of State Tables

F. DOUGLAS SWESTY

Laboratory for Computational Astrophysics, Department of Astronomy & National Center for Supercomputing Applications, University of Illinois at Urbana-Champaign, Urbana, Illinois 61801

Received March 23, 1995; revised February 15, 1996

We present a method for constructing a thermodynamically consistent bi-quintic interpolation scheme that permits the construction of accurate equation of state (EOS) tables. Thermodynamic consistency requires that the first law of thermodynamics be satisfied exactly, i.e., that the pressure and entropy must satisfy the appropriate Maxwell relations. Furthermore, the pressure and internal energy must satisfy their definitions in terms of the derivatives of the Helmholtz free energy. We delineate in this paper a method of high-order interpolation in tables of the Helmholtz free energy, and its derivatives with respect to density and temperature, that ensures that both of these consistency conditions are exactly satisfied. This technique is capable of building highly accurate and consistent EOS tables as a function of temperature and density for use in numerical simulations of reactive flows where the maintenance of thermodynamic consistency is critical. In addition, this method of interpolation maintains continuity of the derivatives of pressure and internal energy with respect to density and temperature. This formalism can be extended to the case where the EOS is a function of chemical composition variables as well as density and temperature.

1. INTRODUCTION

Tabular equations of state have often been used in the numerical hydrodynamic and hydrostatic modeling of astrophysical phenomena. Usually, the use of EOS (equation of state) tables has been motivated by the fact that the computer codes for the direct numerical evaluation of the EOS are overly time consuming, unstable, or in some way unsuitable for incorporation into a numerical hydrodynamic or radiation-hydrodynamic simulation.

One can easily think of many examples of cases where direct calculation of the EOS is extremely complex. This complexity often arises from the need to solve the many body problem in some approximation in order to describe the interactions among the constituents of the gas or liquid. Such calculations of the EOS may require the direct solution of sets of highly non-linear chemical and pressure equilibrium equations, or the variational solution of Hartree–Fock or Thomas–Fermi equations, or they may indirectly involve lattice and molecular dynamics simulations to correctly describe the behavior of matter. Obviously many of these approaches are highly impractical for use in the course of a radiation-hydrodynamic simulation because the numerical evaluation of such complex equations of state are computationally prohibitive. In some cases, such as lattice simulations or in molecular dynamics simulations, the evaluation of the internal energy and pressure at a single density and temperature may require more computational effort than an entire radiation hydrodynamic simulation.

In addition to calculational difficulties, the EOS may exhibit a wide range of behavior over the range of temperature and density that one is interested in. Such behavior may manifest itself as sharp discontinuities in thermodynamic variables near phase transitions and coexistence boundaries. When the EOS is based on theory it may rely on different underlying physical models or calculational techniques in different ranges of temperature and density. This is particularly true for multi-phase chemical equilibrium models for the EOS, such as liquid drop models for dense matter, where the matching of pressures and energies at phase boundaries can be very difficult (see [1] for an example). In numerical hydrodynamics codes it is often advantageous to have a tabular interpolation scheme "smooth" away discontinuities in EOS tables. Even small discontinuities in the pressure or internal energy on order of $\sim 10^{-5}$, which are not physically significant, can pose numerical problems for the implicit solution of hydrodynamic equations which are often solved by means of Newton–Raphson iteration. In the case of a phase transition, smoothing of the EOS table may mean that the discontinuities in physical variables are replaced by a continuous transition. However, by refining the table near the phase boundary this transition could be made arbitrarily sharp. While for some applications this may be unacceptable, for many applications, such as those utilizing implicit numerical techniques, this may not only be acceptable but necessary as well. The scheme we propose in this paper is also designed to address this need.

Last, the method of direct calculation of the EOS itself

0021-9991/96 $18.00

may be plagued by numerical pathologies which may be encountered at a particular density and temperature. This is true in chemical equilibrium models for the EOS which may rely on Newton–Raphson iteration to solve sets of highly non-linear chemical equilibrium equations. If the equations are pathological in certain neighborhoods of the density–temperature plane or if one makes a bad initial guess of the iterative variables the Newton–Raphson scheme may fail to converge and thus a hydrodynamic simulation comes to a jarring halt.

For these reasons, the use of tables to describe the EOS is highly desirable in many cases. However, the use of tables brings about a different set of difficulties. These difficulties include the need for accuracy in interpolations, the need to achieve sufficient resolution of the behavior of thermodynamic variables, and the need for the interpolated values of the EOS to be thermodynamically consistent. The latter problem is particularly troubling in many cases where reactive flows need to be simulated over very long timescales. This is particularly true in astrophysics where phenomena such as supernovae require simulations to be carried out over 10^4–10^5 timesteps and where the amount of radiation–matter interaction may be particularly sensitive to the entropy of matter. Thermodynamic inconsistency may become manifest via the unphysical buildup of entropy, or temperature, during the numerical simulation of what should be an adiabatic flow. Thus any EOS table must produce internal energies and pressures that not only exhibit fidelity to the true energies and pressures, but the internal energies and pressures themselves must be thermodynamically self-consistent. By the use of the phrase ''thermodynamic consistency'' we refer to how well the EOS satisfies the constraints posed by Maxwell relations of thermodynamics. We will discuss these constraints in the next section.

In this paper we present a scheme for constructing high-order interpolated tabular equations of state in a fashion that ensures thermodynamic consistency and continuity of the derivatives of pressure and internal energy. In Section 2 we establish the criterion for thermodynamic consistency. In Section 3 we present the interpolation scheme and demonstrate that it satisfies the consistency constraints. In Section 4 we present an example calculation utilizing our scheme and an inconsistent scheme for tabular EOS interpolation. In Section 4 we offer some conclusions about the use of this scheme and the extensions to higher dimensional interpolations.

2. THERMODYNAMIC CONSISTENCY

As we have already mentioned, any attempt to produce tabular equations of state must satisfy the constraints which enforce thermodynamic consistency as well as maintaining accuracy. This constraint has two parts. First, the interpolation scheme must ensure that the first law of thermodynamics can be represented by an exact differential equation (see [2] for a definition of exactness). For a reversible system the first and second laws of thermodynamics require

$$dE = TdS + \frac{P}{n^2}\,dn, \tag{1}$$

where E is the internal energy per particle, S is the entropy per particle, and n is the particle number density. For many hydrodynamic applications, particularly in astrophysics, it is more suitable to employ the temperature, T as a variable as opposed to the entropy S. The appropriate thermodynamic potential is the Helmholtz free energy F which is defined by

$$F = E - TS. \tag{2}$$

By restating Eq. (1) in terms of F we arrive at the relationship between F, T, and n:

$$dF = -SdT + \frac{P}{n^2}\,dn. \tag{3}$$

The entropy and pressure can be defined as

$$S = -\left.\frac{\partial F}{\partial T}\right|_n \tag{4}$$

and

$$P = n^2 \left.\frac{\partial F}{\partial n}\right|_T. \tag{5}$$

Thermodynamics demands that Eq. (3) be an *exact* differential equation in order that the internal energy E and the Helmholtz free energy F be state functions of T and n [3]. In turn, the exactness of Eq. (1) requires that the pressure and entropy satisfy the Maxwell relation

$$-\left.\frac{\partial S}{\partial n}\right|_T = \frac{1}{n^2}\left.\frac{\partial P}{\partial T}\right|_n. \tag{6}$$

The second constraint that the pressure and entropy must satisfy are their definitions in terms of the Helmholtz free energy per particle F. Thus any tabular EOS should also satisfy Eqs. (4) and (5). We will demonstrate numerically in Section 4 that the failure to satisfy these thermodynamic constraints in numerical simulations leads to unphysical entropy production or loss in otherwise adiabatic flows.

3. THE THERMODYNAMICALLY CONSISTENT INTERPOLATION SCHEME

A fundamental assumption that we make in discussing the following method of interpolation is that one knows the value of the Helmholtz free energy and its derivatives with respect to density and temperature at an orthogonal grid of points (T_i, n_j) covering a region of the $n - T$ plane which is of interest. This essentially specifies a global "model" for the free energy. The knowledge of the derivatives relates directly to the knowledge of the pressure and entropy at the grid points because of Eqs. (4) and (5). Alternatively, one may know the values of the internal energy at the grid points. The Helmholtz free energy can then be calculated using Eq. (2) and the knowledge of S at the grid points. However, one cannot consistently specify both the free energy F and the internal energy E along with S unless the values satisfy Eq. (2) in which case the knowledge of F and S is equivalent to the knowledge of E and S.

Given that we possess the knowledge of the value of F as well as $\partial F/\partial n$ and $\partial F/\partial T$, we would like to be able to calculate the values of F, E, P, and S at intermediate points in the $n - T$ plane in a manner that maintains fidelity to the global behavior of the data known at the grid points and that satisfies the thermodynamic relationships given by Eqs. (4), (5), and (6). Let us consider an arbitrary value of n and T in the rectangular cell of the density-temperature plane bounded by the grid points (n_i, T_j), (n_{i+1}, T_j), (n_i, T_{j+1}), and (n_{i+1}, T_{j+1}). One way to assure thermodynamic consistency is to explicitly construct the pressure and entropy from the analytic function which describes the free energy in this region via Eqs. (4) and (5). The commutability of partial derivatives with respect to n and T, i.e.,

$$\frac{\partial^2 F}{\partial T \partial n} = \frac{\partial^2 F}{\partial n \partial T}, \tag{7}$$

thus guarantees that the Maxwell relation (6) will be satisfied also. Thus, thermodynamic consistency is ensured as long as the pressure and entropy are calculated by applying Eqs. (4) and (5) to the free energy interpolation function and by calculating E using Eq. (2) *regardless of the particular choice of interpolation method.*

In addition to thermodynamic consistency we desire that the interpolation between grid points have several other attributes. The first of these is fidelity of the interpolation to the underlying thermodynamic data in the table. We wish F to go to the correct values as one approaches a grid point, i.e., that

$$F \to F(T_i, n_j) \tag{8}$$

as $(T, n) \to (T_i, n_j)$. Similarly, we wish the derivatives of F to exhibit a similar limiting behavior,

$$\frac{\partial F}{\partial T} \to \left.\frac{\partial F}{\partial T}\right|_{ij} \tag{9}$$

and

$$\frac{\partial F}{\partial n} \to \left.\frac{\partial F}{\partial n}\right|_{ij} \tag{10}$$

as $(T, n) \to (T_i, n_j)$. This assures that the pressure, entropy, and internal energy also obtain the correct values as the grid point is approached. Additionally, we wish the second derivatives of F to tend to the correct values as a grid point is approached,

$$\frac{\partial^2 F}{\partial T^2} \to \left.\frac{\partial^2 F}{\partial T^2}\right|_{ij} \tag{11}$$

and

$$\frac{\partial^2 F}{\partial n^2} \to \left.\frac{\partial^2 F}{\partial n^2}\right|_{ij} \tag{12}$$

as $(T, n) \to (T_i, n_j)$ which ensures that derivatives such as $\partial E/\partial T$, $\partial E/\partial n$, $\partial P/\partial T$, etc. attain the correct values as the grid point is approached. This requirement is not motivated by any thermodynamic considerations. Rather, it is motivated by the considerations of numerical hydrodynamics, where discontinuities in the derivatives of the pressure and internal energy with respect to density and temperature often cause numerical difficulties in the solution of the Euler equations. Experience has shown us that if one implements only the constraints described by Eqs. (8), (9), and (10) the resulting discontinuity of the derivatives of the pressure and internal energy at a grid point is more than sufficient to wreak havoc on Newton–Raphson iteration schemes that are used to solve an implicitly finite-differenced gas energy equation. By insisting on the constraints in the interpolation equations described by Eqs. (11) and (12) we avoid this problem. Finally, we wish the interpolation function and its first and second derivatives to remain continuous as we cross the boundary from one cell into another in the mesh of grid points that covers the region of the temperature density plane that is of interest.

Other existing EOS interpolation schemes such as the monotone piecewise bi-cubic scheme of Carlson and Fritsch [4] (hereafter CF) do not specifically attempt to address the concern of maintaining thermodynamic consistency in the interpolation. The CF scheme requires the use of separate interpolations for the pressure and internal energy and does not assure their consistency. While in many circumstances the CF scheme, when applied to a

given set of data, provides enough accuracy in the interpolation to assure that thermodynamic inconsistency is kept to an acceptable level our intent is to create an interpolation scheme that *guarantees* thermodynamic consistency. In addition, the CF scheme is designed primarily to maintain monotonicity in the interpolation in a monotonic data set. However, there are situations, in astrophysics, for example [1, 5], where the internal energy per particle is not a monotonic function of density and where pressure is not a monotonic function of the temperature. In these cases the preservation of monotonicity in the behavior of the internal energy per particle as a function of n or the pressure as a function of T becomes irrelevant. We provide an example of such an equation of state in Section 4. We wish to point out that thermodynamic stability does require [3]

$$\left.\frac{\partial S}{\partial T}\right|_n > 0, \tag{13}$$

$$\left.\frac{\partial P}{\partial n}\right|_T > 0, \tag{14}$$

and

$$\left.\frac{\partial P}{\partial n}\right|_S > 0. \tag{15}$$

The scheme that we propose below does not explicitly guarantee that the constraints posed by Eqs. (13)–(15) are satisfied. We would also like to point out that the CF scheme does not satisfy the constraint posed by Eq. (15). For the interpolation scheme we describe below it is necessary to verify by numerical inspection that these constraints are satisfied for each individual application of this scheme. In some cases enforcing thermodynamic stability may involve the judicious choice of the locations of the mesh points in order to resolve sharp phenomena and ensure that Eqs. (13)–(15) are satisfied. In practice, using equations of state for astrophysical interest, we have never encountered a situation where thermodynamic instabilities occur in the interpolated values of S and P.

Another point which we would like to make involves the many numerical methods for hydrodynamic simulations [6, 7] that rely on Riemann solvers in order to simulate the flow of fluids. However, some approximate Riemann solvers [8] employed in these methods require convexity of the EOS which places an additional constraint on the EOS [9]:

$$\left.\frac{\partial^2 P}{\partial V^2}\right|_S > 0, \tag{16}$$

where $V = 1/n$. This condition may not be satisfied in a realistic EOS in regions near phase transitions (for an example of this see [1]). For this reason we do not attempt to enforce the constraint posed by Eq. (16) in our interpolation scheme. If one wishes to apply the scheme we define below to an EOS which satisfies Eq. (16) everywhere in domain of interest then compliance with this constraint must be verified by numerical inspection. Note that the CF scheme does not satisfy Eq. (16). Finally, we wish to note that the stability of shock waves in two dimensions may place further constraints on the EOS (see Section VII of [9] for a discussion). Neither our scheme or the CF scheme attempts to satisfy these constraints.

It would be desirable to formulate a scheme that also ensured thermodynamic stability. However, given that we require thermodynamic consistency, fidelity to the underlying data, and continuity of the quantities E, S, and P, and their derivatives with respect to T and n, this would, at a minimum, require an interpolation scheme that contains more parameters then the bi-quintic scheme described in the remainder of this section. Even when considering quintic interpolation in only one variable, the six coefficients of the Hermite basis functions, which we describe in a subsequent paragraph, are determined by the properties of thermodynamic consistency, fidelity to the data, and the continuity of the thermodynamic functions and their derivatives. Furthermore, it is unclear how the parameters in a higher order scheme could be chosen so as to ensure thermodynamic stability. For this reason we address only the properties of thermodynamic consistency, fidelity to the underlying data on the grid points, and continuity of the thermodynamic variables in the remainder of this paper.

In this paper we will avoid the issue of what mesh spacing is needed to accurately represent the EOS itself. This will depend on the specifics of the particular EOS one wants to represent as a table. Clearly, an EOS in which the thermodynamic state functions are slowly varying functions of temperature and density will require fewer grid points to adequately represent the EOS then will one with rapidly varying state functions. We leave the specifics of the choice mesh spacing up to the reader.

In order to construct an interpolation scheme in two dimensions that possesses the aforementioned required properties, we first consider the interpolation of F between two temperature points, T_i and T_{i+1}, at a fixed density n_j. The Helmholtz free energy can be constructed at intermediate temperatures in a manner which has the desired properties by means of piecewise quintic Hermite interpolation [10]:

$$\begin{aligned}\tilde{F}(T, n_j) = {} & F^i(n_j)\psi_x^0 + F^{i+1}(n_j)\psi_{1-x}^0 + F_T^i(n_j)\psi_x^1 \\ & - F_T^{i+1}(n_j)\psi_{1-x}^1 + F_{TT}^i(n_j)\psi_x^2 + F_{TT}^{i+1}(n_j)\psi_{1-x}^2,\end{aligned} \tag{17}$$

where the ψ functions are the quintic Hermite basis functions given by

$$\psi_z^0 = \psi^0(z) = -6z^5 + 15z^4 - 10z^3 + 1, \tag{18}$$

$$\psi_z^1 = \psi^1(z) = -3z^5 + 8z^4 - 6z^3 + z, \tag{19}$$

and

$$\psi_z^2 = \psi^2(z) = \tfrac{1}{2}(-z^5 + 3z^4 - 3z^3 + z^2) \tag{20}$$

and where x is defined by

$$x \equiv \frac{T - T_i}{T_{i+1} - T_i}. \tag{21}$$

We also define the coefficients F_T and F_{TT} by

$$F_T^l \equiv \left.\frac{\partial F}{\partial T}\right|_l (T_{i+1} - T_i) \tag{22}$$

and

$$F_{TT}^l \equiv \left.\frac{\partial^2 F}{\partial T^2}\right|_l (T_{i+1} - T_i)^2, \tag{23}$$

where $l = i$ or $l = i + 1$. The fact that the correct limit of $\tilde{F}$ and its first and second derivatives with respect to T obtains as $T \to T_{\rm i}$, T_{i+1} can be verified by simple algebra. Note the minus sign in the fourth term of Eq. (17) which is necessary in order to ensure that the sign of $\partial\tilde{F}/\partial T$ is correct as $T \to T_{i+1}$. The quintic Hermite basis functions are chosen so as to ensure that all the terms of $\tilde{F}$ but the one containing ψ^0 vanish as $x \to 0$. If one takes the first derivative of Eq. (17) the only surviving term is the one involving $\partial\psi_x^1/\partial T$ as $x \to 0$. The second derivative of $\tilde{F}$ exhibits similar behavior.

This interpolation scheme can easily be extended to two dimensions by interpolating each of the coefficients of the basis functions in the density n using the same quintic interpolation scheme that we applied in order to interpolate F in T. The resulting bi-quintic interpolation function for F in the temperature-density rectangle bounded by (T_i, n_j) and (T_{i+1}, n_{j+1}) is given by

$$\begin{aligned}
\tilde{F}(T,n) = {} & F^{i,j}\psi_x^0\psi_y^0 + F^{i+1,j}\psi_{1-x}^0\psi_y^0 + F^{i,j+1}\psi_x^0\psi_{1-y}^0 \\
& + F^{i+1,j+1}\psi_{1-x}^0\psi_{1-y}^0 + F_T^{i,j}\psi_x^1\psi_y^0 - F_T^{i+1,j}\psi_{1-x}^1\psi_y^0 \\
& + F_T^{i,j+1}\psi_x^1\psi_{1-y}^0 - F_T^{i+1,j+1}\psi_{1-x}^1\psi_{1-y}^0 + F_{TT}^{i,j}\psi_x^2\psi_y^0 \\
& + F_{TT}^{i+1,j}\psi_{1-x}^2\psi_y^0 + F_{TT}^{i,j+1}\psi_x^2\psi_{1-y}^0 + F_{TT}^{i+1,j+1}\psi_{1-x}^2\psi_{1-y}^0 \\
& + F_n^{i,j}\psi_x^0\psi_y^1 + F_n^{i+1,j}\psi_{1-x}^0\psi_y^1 - F_n^{i,j+1}\psi_x^0\psi_{1-y}^1 \\
& - F_n^{i+1,j+1}\psi_{1-x}^0\psi_{1-y}^1 + F_{nn}^{i,j}\psi_x^0\psi_y^2 + F_{nn}^{i+1,j}\psi_{1-x}^0\psi_y^2 \\
& + F_{nn}^{i,j+1}\psi_x^0\psi_{1-y}^2 + F_{nn}^{i+1,j+1}\psi_{1-x}^0\psi_{1-y}^2 + F_{Tn}^{i,j}\psi_x^1\psi_y^1 \\
& - F_{Tn}^{i+1,j}\psi_{1-x}^1\psi_y^1 - F_{Tn}^{i,j+1}\psi_x^1\psi_{1-y}^1 + F_{Tn}^{i+1,j+1}\psi_{1-x}^1\psi_{1-y}^1 \\
& + F_{TTn}^{i,j}\psi_x^2\psi_y^1 + F_{TTn}^{i+1,j}\psi_{1-x}^2\psi_y^1 - F_{TTn}^{i,j+1}\psi_x^2\psi_{1-y}^1 \\
& - F_{TTn}^{i+1,j+1}\psi_{1-x}^2\psi_{1-y}^1 + F_{Tnn}^{i,j}\psi_x^1\psi_y^2 - F_{Tnn}^{i+1,j}\psi_{1-x}^1\psi_y^2 \\
& + F_{Tnn}^{i,j+1}\psi_x^1\psi_{1-y}^2 - F_{Tnn}^{i+1,j+1}\psi_{1-x}^1\psi_{1-y}^2 + F_{TTnn}^{i,j}\psi_x^2\psi_y^2 \\
& + F_{TTnn}^{i+1,j}\psi_{1-y}^2\psi_y^2 + F_{TTnn}^{i,j+1}\psi_x^2\psi_{1-y}^2 + F_{TTnn}^{i+1,j+1}\psi_{1-x}^2\psi_{1-y}^2,
\end{aligned} \tag{24}$$

where we have defined y by

$$y \equiv \frac{n - n_j}{n_{j+1} - n_j}. \tag{25}$$

In Eq. (24) the coefficients are defined by

$$F_n^{lk} \equiv \left.\frac{\partial F}{\partial n}\right|_{lk} (n_{j+1} - n_j), \tag{26}$$

$$F_T^{lk} \equiv \left.\frac{\partial F}{\partial T}\right|_{lk} (T_{i+1} - T_i), \tag{27}$$

$$F_{nn}^{lk} \equiv \left.\frac{\partial^2 F}{\partial n^2}\right|_{lk} (n_{j+1} - n_j)^2, \tag{28}$$

$$F_{TT}^{lk} \equiv \left.\frac{\partial^2 F}{\partial T^2}\right|_{lk} (T_{i+1} - T_i)^2, \tag{29}$$

$$F_{Tn}^{lk} \equiv \left.\frac{\partial^2 F}{\partial T \partial n}\right|_{lk} (T_{i+1} - T_i)(n_{j+1} - n_j), \tag{30}$$

$$F_{TTn}^{lk} \equiv \left.\frac{\partial^3 F}{\partial T^2 \partial n}\right|_{lk} (T_{i+1} - T_i)^2(n_{j+1} - n_j), \tag{31}$$

$$F_{Tnn}^{lk} \equiv \left.\frac{\partial^3 F}{\partial T \partial n^2}\right|_{lk} (T_{i+1} - T_i)(n_{j+1} - n_j)^2, \tag{32}$$

$$F_{TTnn}^{lk} \equiv \left.\frac{\partial^4 F}{\partial T^2 \partial n^2}\right|_{lk} (T_{i+1} - T_i)^2(n_{j+1} - n_j)^2, \tag{33}$$

where $l = i, i + 1$ and $k = j, j + 1$. Despite the fact that Eq. (24) contains 36 terms, the repetitive patterns present in the structure terms make it possible to easily translate into computer code. As in the one-dimensional case with simple, but tedious, algebra one can easily verify that this interpolative formula and its first and second derivatives maintain the behavior we desire as $(T, n) \to (T_i, n_j)$. Note that the two-dimensional interpolation contains cross

terms involving derivatives of second and higher order. It has been pointed out [11] that the last three lines of Eq. (24) are not necessary in order to ensure that $\tilde{F}$ and its derivatives obtain the proper values at the grid points or to ensure smoothness across cell boundaries. However, in practice the addition of the third- and fourth-order derivatives that make up the last three lines of Eq. (24) ensures that the value of $\partial^2\tilde{F}/\partial T^2$ and $\partial^2\tilde{F}/\partial n^2$ remain well behaved in the middle of a cell. By experience we have found that the omission of these terms can allow the second derivatives of $\tilde{F}$ to exhibit unphysical and undesirable oscillations as one moves through the center of a cell.

This interpolation scheme could be extended to higher dimensions in the same fashion that it was extended from one to two dimensions. However, because of the explosion in the number of terms (216) to go to three dimensions we will not consider this situation further in this work.

One matter we wish to comment on is the second and higher order derivatives of the Helmholtz free energy needed in Eqs. (17) and (24). If one does not directly know the values of the higher order derivatives of F all is not lost as they can sometimes be calculated by finite differencing of the free energy or lower order derivative values at adjacent grid points. This is sufficient to assure continuity of the derivatives of the pressure and internal energy. However, we do not recommend this approach as we have experienced problems maintaining local monotonicity in the second derivatives of $\tilde{F}$ in some cases when we adopt such an approach. The problems originate with the difficulty of accurately representing the second and higher order derivatives using a finite-difference approximation based on the lower order derivatives at the mesh points. While it will obviously depend on the specific EOS, in some cases such finite-difference approximations to these derivatives may involve a very inaccurate value for the derivative. Where it is possible we recommend the use of accurate values for the high order derivatives of F.

As a final comment, we wish to point out that if speed or computer memory limitations are considerations other lower order schemes will likely be faster or less memory intensive. Clearly the number of floating-point operations involved in evaluating the terms of Eq. (24) will be larger than those required of a simpler interpolation scheme. Similarly, a simpler interpolation function will be less memory intensive than the scheme we have described above. For example, the two separate interpolations for E and P in the CF scheme require the storage of six pieces of data at each grid point, in contrast to the nine pieces our scheme requires. However, our motivation for developing this scheme was to provide an interpolation method for applications where the maintenance of thermodynamic consistency and the continuity of derivatives of the thermodynamic functions are of paramount concern.

4. AN ILLUSTRATIVE CALCULATION

In this section we provide an illustration of the use of the interpolation technique that we have described in the previous section. We wish to show in a concrete fashion the properties of the interpolation and to demonstrate the thermodynamic consistency. In order to do this we will consider the equation of state of a relativistic electron-positron gas which often is utilized in describing astrophysical phenomena. While this EOS has a simple analytic formulation, we employ it here to provide an example of how the interpolation technique works.

The EOS has been described elsewhere [1] and we simply repeat the essential results here. The Helmholtz free energy per particle is given by

$$F = \frac{1}{4\pi^2 n(\hbar c)^3}\left(\mu^4 + \frac{2}{3}\pi^2 T^2\mu^2 - \frac{7}{45}\pi^4 T^4\right), \quad (34)$$

where μ is the chemical potential of the electrons, $\hbar$ is the reduced Planck's constant, and c is the speed of light. The chemical potential is given by

$$\mu = (a+b)^{1/3} - \frac{\pi^2 T^2}{3(a+b)^{1/3}}, \quad (35)$$

where a and b are given by

$$a = \frac{3}{2}\pi^2(\hbar c)^3 n \quad (36)$$

and

$$b = \sqrt{a^2 + \pi^6 T^6/27}. \quad (37)$$

For convenience we work in nuclear units of mega electron volts and Fermis (1 fm $= 10^{-13}$ cm), where $\hbar = 6.5821220 \times 10^{-22}$ MeV$\cdot$s and $c = 2.99792458 \times 10^{23}$ fm$\cdot$s^{-1}. The temperature T is measured in MeV and the entropy in measured in units of Boltzmann's constant k_B which in these units has a value of unity.

Using the electron–positron EOS we constructed a grid of values of F and its derivatives for temperatures in the range $T \in [1, 14]$ MeV and densities in the range $n \in [10^{-6}, 10^{-1}]$ fm^{-3}. This range of temperature and density corresponds to the environment found in a gravitationally collapsing star where the electron–positron EOS is physically relevant [1]. We employed 14 mesh points in the T dimension which were linearly spaced with $T_{i+1} - T_i = 1$ MeV. In the density dimension we employed 51 points which were logarithmically spaced in order to provide 10 mesh points per decade of density. This is a typical spacing

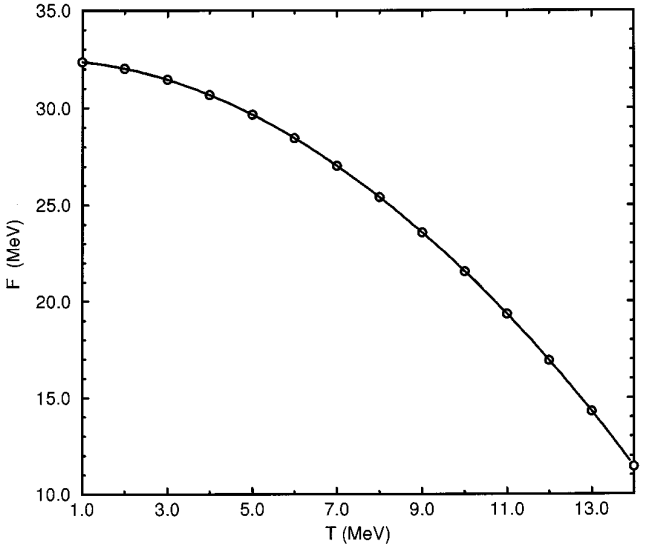

FIG. 1. A density ($n = 3.57 \times 10^{-4}$ fm^{-3}) slice illustrating the properties of the Helmholtz free energy interpolation function. The circles are true values obtained directly from the analytic EOS while the solid line represents the interpolated value.

for an EOS table to be utilized in stellar collapse simulations.

An example of how the interpolation performs can be seen in Figs. 1–10, where the interpolation function $\tilde{F}$ and the derived thermodynamic variables are plotted for a range of temperatures at a constant density $n = 3.57 \times 10^{-4}$ fm^{-3}. This density is an intermediate value located halfway between the 26th and 27th density mesh points. This particular choice of density allows us to depict the interpolated values at an extremal distance from the mesh points. The circles in Figs. 1–10 depict the true values of the plotted functions. As the figures clearly show, the interpolated energies, pressure, entropy, and the corresponding derivatives maintain an excellent global and local agreement with the true values.

An example of the manifestation of thermodynamic inconsistency can also be provided with the aforementioned electron–positron EOS. We consider a single zone of a

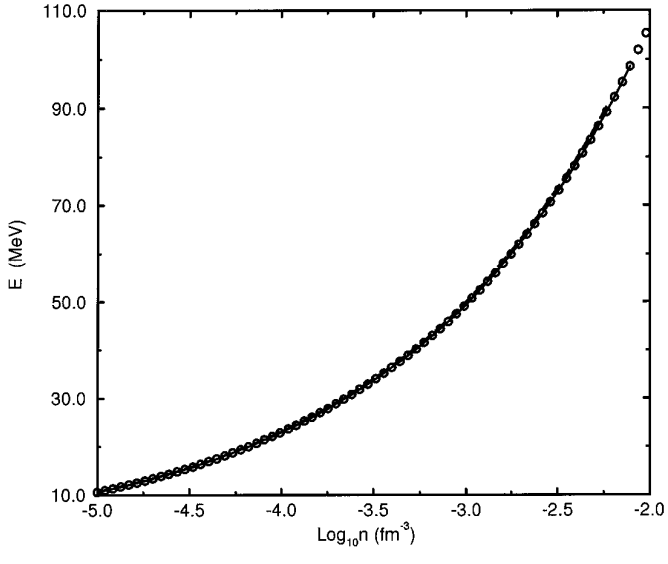

FIG. 2. The internal energy per baryon for the same constant density slice as Fig. 1. The circles are true values obtained directly from the analytic EOS while the solid line depicts the analytic derivative of the interpolation function.

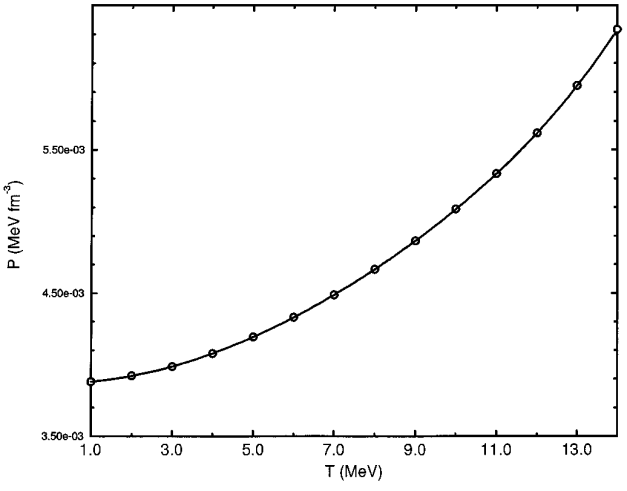

FIG. 3. The same as Fig. 2, except that the pressure is depicted.

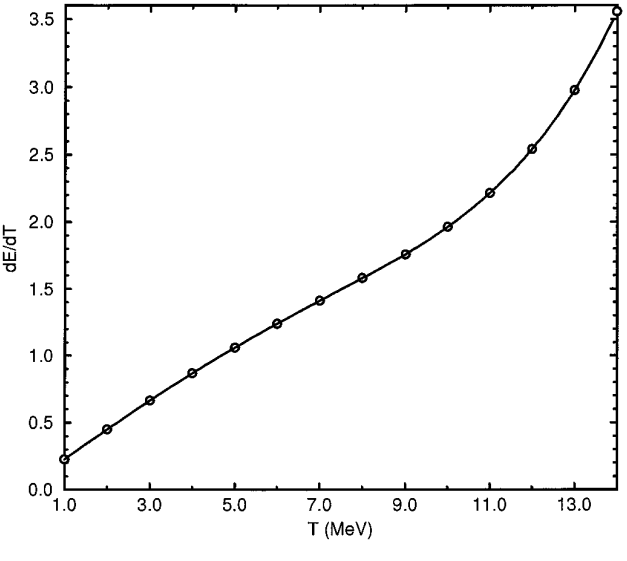

FIG. 4. The same as Fig. 2, except that dE/dT is depicted.

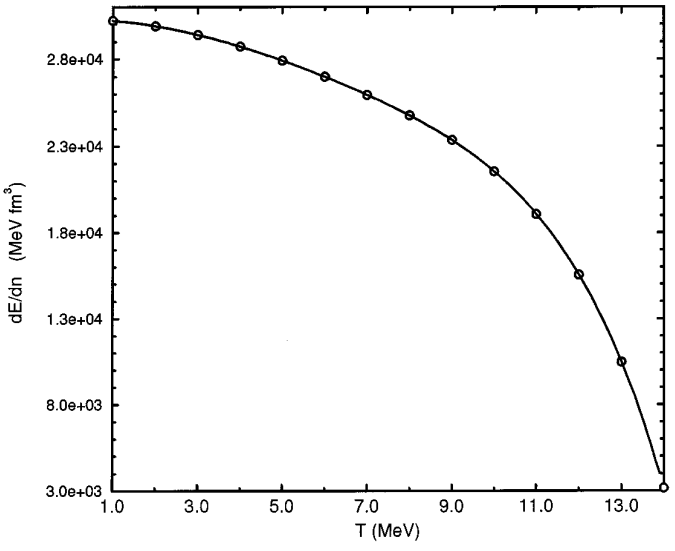

FIG. 5. The same as Fig. 2, except that dE/dn is depicted.

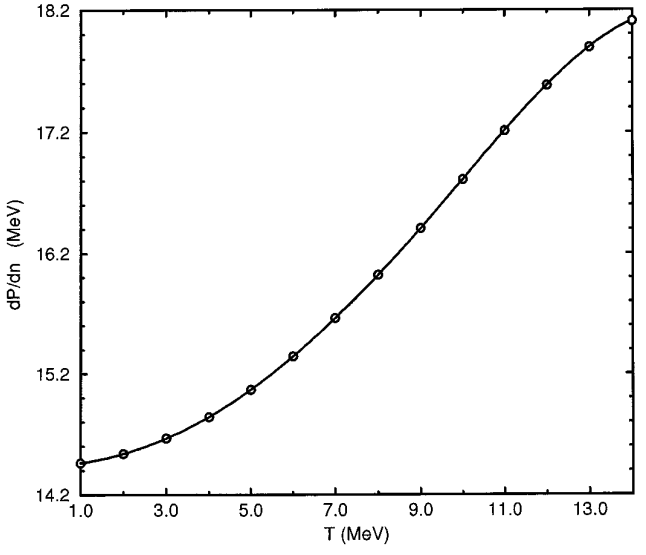

FIG. 7. The same as Fig. 2, except that dP/dn is depicted.

Lagrangean fluid dynamics calculation where the first law of thermodynamics is given by

$$dE + Pd\left(\frac{1}{n}\right) = 0 \tag{38}$$

in the absence of heat production or loss. We simulate the compression of this single zone, or fluid element, by time-evolving this equation in a standard implicit Crank–Nicholson (time-centered) finite-difference fashion,

$$E^{m+1} - E^m + \frac{1}{2}(P^{m+1} + P^m)\left[\frac{1}{n^{m+1}} - \frac{1}{n^m}\right] = 0, \tag{39}$$

where the superscript m is the standard finite-difference notation for the time level. In Eq. (39) both E^{m+1} and P^{m+1} are functions of the temperature at the new time level T^{m+1}, making this equation an implicit function of T^{m+1}. We evolve the equation by gently compressing the density by one percent per timestep, i.e.,

$$n^{m+1} = 1.01n^m. \tag{40}$$

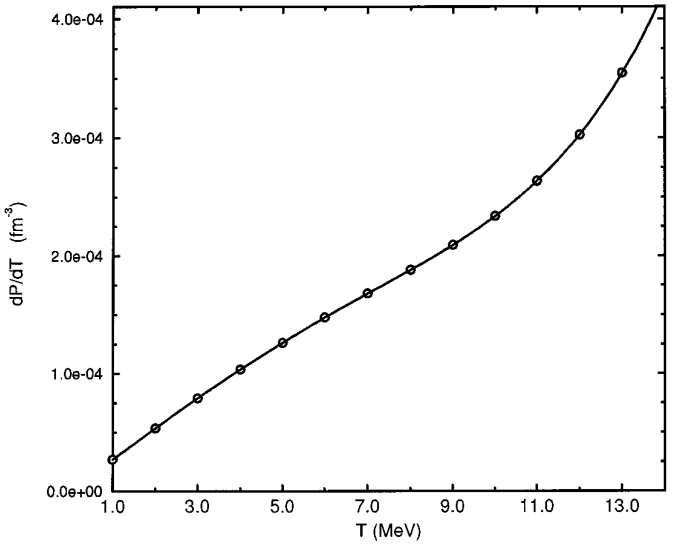

FIG. 6. The same as Fig. 2, except that dP/dT is depicted.

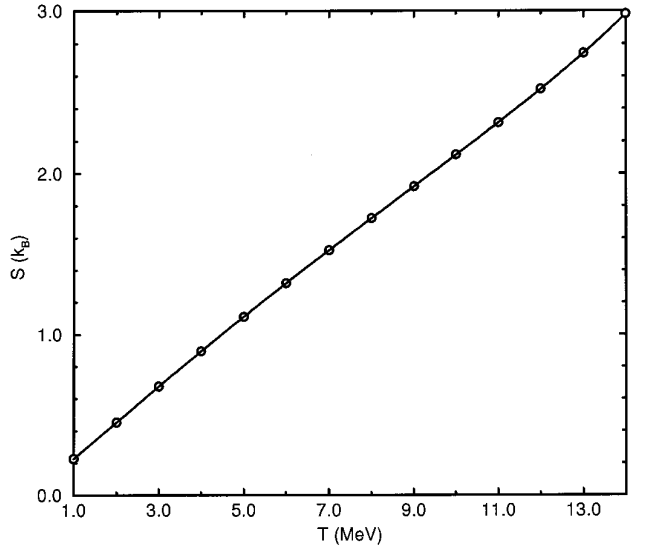

FIG. 8. The same as Fig. 2, except that the entropy is depicted.

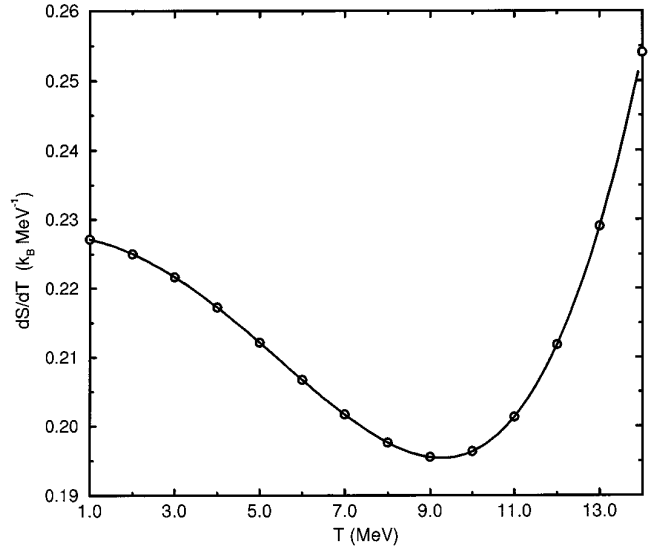

FIG. 9. The same as Fig. 2, except that dS/dT is depicted.

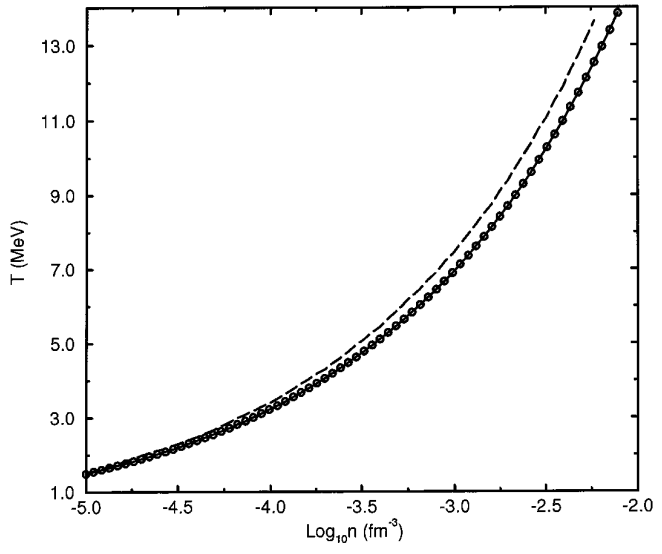

FIG. 11. The temperature versus density for the energy equation example. The circles are the true adiabatic solution, the solid line depicts the result using the bi-quintic free energy interpolation method while the dashed line illustrates the result found using bilinear interpolation on the same mesh.

The new value of T^{m+1} is then found by finding the root of Eq. (39) using Newton–Raphson iteration.

For such a slow increase in the density of a fluid element the compression should be adiabatic if there are no thermodynamic inconsistencies present in the EOS. In Fig. 11 we illustrate the results of the aforementioned simulation. We began the simulation at $T = 1$ MeV and $n = 10^{-5}$ fm^{-3} and ran the calculation for approximately 650 timesteps which is when the temperature ran off the upper edge of the grid. In Fig. 11 we compare the true adiabatic solution (circles) to the results of the simulation using the bi-quintic interpolation (solid line). As is apparent from Fig. 11 the agreement between the true solution and the simulation using the bi-quintic technique is excellent.

We have also conducted this simulation using separate bilinear interpolations in E and P on the same mesh in order to provide an illustration of the buildup of thermodynamic inconsistency. The use of separate interpolations for E and P introduces thermodynamic inconsistencies which in this case manifest themselves by moving the $T - n$ trajectory of the compression away from the adiabat. After compression of the fluid element by three decades of density the temperatures along the two curves differ by nearly $\Delta T \approx 1.1$ MeV or nearly 10%. In order to ascertain that the result was numerically stable we reduced the density increase to one-tenth of a percent per timestep a found virtually identical trajectories.

In stellar collapse simulations where infalling gas may be compressed by as much as five orders of magnitude in density the resulting temperature error could completely invalidate a numerical simulation. This may be true in other reactive flow situations, where reaction rates are very sensitive to the temperature.

To be fair, we wish to point out that for the simple equation of state we have employed in this example one could utilize separate bi-linear interpolations in log E and log P that would give rise to only a minimal amount of thermodynamic inconsistency since both the pressure and internal energy for this particular EOS have approximately power-law behavior as a function of density and temperature. For a more general EOS this would not be true and such schemes may not work well. One could argue that it

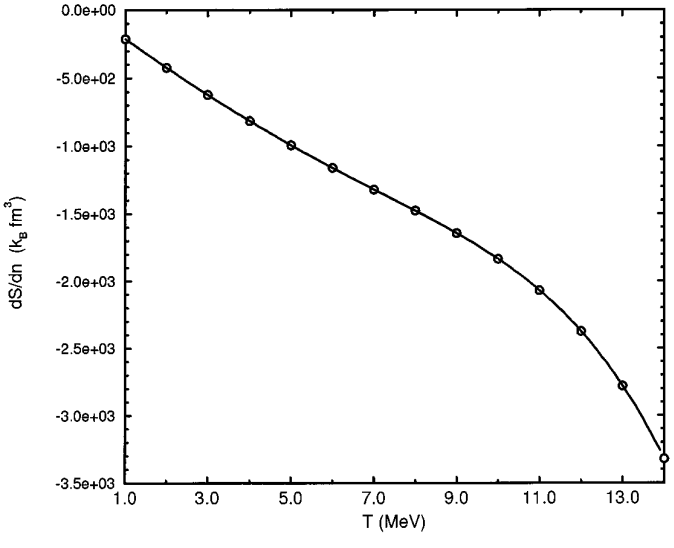

FIG. 10. The same as Fig. 2, except that dS/dn is depicted.

is always possible to minimize the problem for a particular EOS by refining the table until sufficient thermodynamic consistency is achieved. Our intent here is to provide an alternative to such ''tuning.'' Note that bi-linear interpolation would yield discontinuous derivatives of the pressure and internal energy which would create problems for implicit hydrodynamics codes. One would have to utilize at least a bi-cubic scheme to assure continuity of the derivatives of the pressure and energy.

We have not employed the CF monotonic interpolation scheme in this example since the internal energy per particle is not a globally monotonic function of density for the electron–positron EOS for densities and temperatures employed in this example. In all fairness, in cases where the energy and pressure are monotonic functions of density and temperature the CF scheme may be sufficient to accurately represent the EOS without introducing unacceptable levels of thermodynamic inconsistency. In contrast, our intent in this paper has been to develop an accurate scheme which guarantees thermodynamic consistency as well as the continuity of the derivatives of E and P in all cases.

5. CONCLUSIONS

In this paper we have developed a bi-quintic thermodynamically consistent interpolation scheme capable of representing EOS data in numerical hydrodynamic simulations. This scheme has been developed to satisfy three main criteria. The first criterion is that the interpolation method must be thermodynamically consistent. The second is that the interpolation scheme must faithfully reproduce the underlying data in the table. And the final criterion is the derivatives of the internal energy per particle and pressure with respect to the density and temperature must be continuous and well behaved.

The bi-quintic Hermite interpolation scheme we have developed guarantees thermodynamic consistency by interpolating in the Helmholtz free energy using knowledge of the values of the free energy and its first and second derivatives to determine the coefficients of the Hermite basis functions. This ensures that the interpolation function and its derivatives remain faithful to the original data. The thermodynamic variables E, P, and S are then constructed directly from the free energy interpolation by taking analytic derivatives of the free energy functional thereby ensuring that they obey the appropriate Maxwell relations as well as satisfy the original definitions in terms of the free energy. We have demonstrated the behavior in this scheme in a sample calculation which illustrates the manifestation of thermodynamic inconsistencies in a hydrodynamic calculation.

While the scheme we have presented herein is devised for a two-dimensional interpolation in the $n - T$ plane, this technique could easily be extended to higher dimensions where the free energy is a function of additional parameters such as chemical composition variables. The only cost in extending the scheme is the growth on the number of terms in the interpolation functional. Adding quintic interpolation would produce $6 \times 36 = 216$ terms in the interpolation functional, instead of the 36 terms present in the two-dimensional case. In many situations linear interpolation in higher dimensions may be sufficient to resolve the problem.

We especially thank Jim Lattimer for his helpful analysis of this technique and his insight into the behavior of Eq. (24). We also thank Dimitri Mihalas and Mike Norman for their suggestions and advice on this project. We acknowledge financial support for this work from the NSF through an NSF Computational Science and Engineering Fellowship (NSF Grant ASC-9308955), from a NASA astrophysics theory grant (NAG 5-3099), and through the Laboratory for Computational Astrophysics (NSF Grant AST-9201113). We also thank the National Center for Supercomputing Applications for computing support.

REFERENCES

1. J. M. Lattimer and F. D. Swesty, *Nucl. Phys. A* **535,** 331 (1991).
2. M. Braun, *Differential Equations and Their Applications* (Springer-Verlag, New York, 1975).
3. H. B. Callen, *Thermodynamics* (Wiley, New York, 1960).
4. R. E. Carlson and F. N. Fritsch, *SIAM J. Numer. Anal.* **22,** 386 (1985).
5. J. M. Lattimer, C. J. Pethick, D. G. Ravenhall, and D. Q. Lamb, *Nucl. Phys. A* **432,** 646 (1985).
6. S. K. Godunov, *Math. Sb.* **47,** 357 (1959).
7. P. Colella and P. R. Woodward, *J. Chem. Phys.* **54,** 174 (1984).
8. P. Colella and H. M. Glaz, *J. Chem. Phys.* **59,** 264 (1985).
9. R. Menikoff and B. J. Plohr, *Rev. Mod. Phys.* **61,** 75 (1988).
10. P. J. Davis, *Iterpolation and Approximation* (Dover, New York, 1975).
11. J. Lattimer, personal communication.